

## 2.3 GLOBAL LARGE-SCALE PRECIPITATION: SEASONAL AND INTERANNUAL VARIATIONS IN THE MERGED ANALYSES, REANALYSIS AND NCEP/GFS MODEL OUTPUTS

Pingping Xie<sup>1)\*</sup>, John E. Janowiak<sup>1)</sup>, and Phillip A. Arkin<sup>2)</sup>, Mingyue Chen<sup>3)</sup>

- 1) Climate Prediction Center/NCEP/NOAA
- 2) ESSIC, University of Maryland
- 3) RS Information Systems, Inc.

### 1. INTRODUCTION

In recent years, several sets of high quality data sets of global precipitation have been constructed by combining gauge observations and estimates derived from satellite observations (Huffman et al. 1997, Xie and Arkin 1997, Adler et al. 2003). Covering a period from 1979 to the present over a global grid of 2.5° lat/lon, these merged analyses have been widely applied in climate analysis, numerical model verifications and hydrological studies.

In this work, we present a description of the seasonal and interannual variations of large-scale precipitation over the globe using two sets of merged analyses and compare them with those in the precipitation fields produced by the NCEP/NCAR reanalysis (Kalnay et al. 1996) and the newly developed NCEP / GFS climate model (Wang et al. 2003).

### 2. THE PRECIPITATION DATA SETS

Two sets of merged analyses of global monthly precipitation are used in this study to examine the seasonal and interannual variations of global precipitation. These are the CPC Merged Analysis of Precipitation (CMAP, Xie and Arkin 1997) and the Version 2 data set of the Global Precipitation Climatology Project (GPCP) monthly analysis (Adler et al. 2003). Two versions of monthly precipitation analyses are included in the CMAP data sets: the analysis defined by merging gauge observations, satellite estimates and the NCEP/NCAR reanalysis precipitation fields (CMAP/A) and that derived from observation-based inputs only (CMAP/O). In this study, the observation-only version of the CMAP (CMAP/O) is examined.

In addition to the two sets of the merged analyses described above, precipitation fields produced by the NCEP/NCAR reanalysis (Kalnay et al. 1996) and the AMIP runs of the NCEP / GFS climate model (Wang et al. 2003) are also included in this intercomparison study.

---

\* Corresponding author: Dr. Pingping Xie, Climate Prediction Center, 5200 Auth Road, #605, Camp Springs, MD 20746; E-mail: [Pingping.Xie@noaa.gov](mailto:Pingping.Xie@noaa.gov)

### 3. SEASONAL VARIATIONS

Seasonal variations of global precipitation are first examined. Shown in fig. 1 and 2 are mean precipitation (mm/day) for the DJF, and JJA periods, respectively, averaged over a 23-year period from 1979 to 2001. The two sets of the merged analyses, the CMAP/O and the GPCP Version 2, present very similar spatial distribution patterns of large-scale precipitation over most of the globe, though differences are observed in smaller scale features and in the magnitude. Overall, the CMAP/O exhibits heavier / less precipitation over tropical / extra-tropical oceanic areas compared to the GPCP Version 2 data set (Gruber et al. 2000).

Significant seasonal variations are observed in the merged analyses. During the DJF period (fig.1), the SPCZ is strong and the ITCZ is relatively weak over the central and eastern Pacific. The mid-latitude storm tracks are connected with the ITCZ in the Southern Hemisphere, while they are more separated in the Northern Hemisphere. During the JJA period (fig.2), the SPCZ is at its weakest, while the ITCZ is strong over both the eastern and western Pacific, with a slight relative minimum observed over its central part.

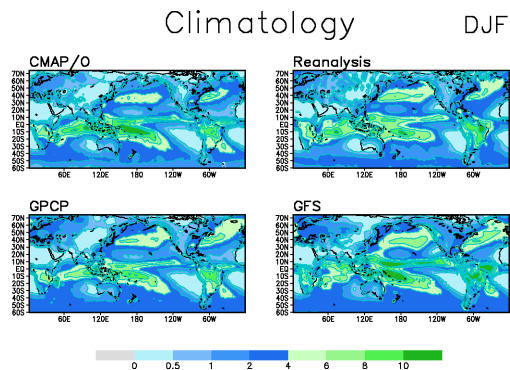


Fig. 1: Mean precipitation (mm/day) for the December-January-February (DJF) period averaged over a 23-year period from 1979 to 2001 for the merged analyses of a) the CMAP/O, and b) GPCP Version 2, and the precipitation fields generated by c) the NCEP/NCAR reanalysis, and d) the NCEP / GFS climate model AMIP runs.

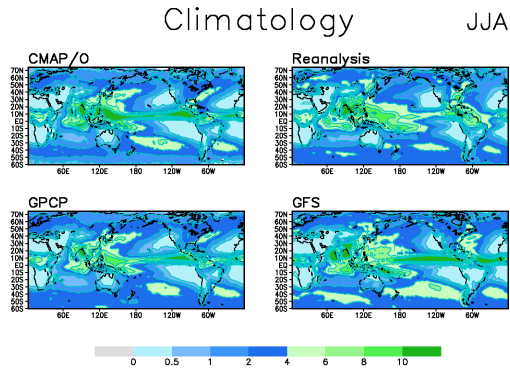


Fig. 2: As in figure 1, except for the June-July-August (JJA) mean precipitation.

In general, both the NCEP / NCAR reanalysis and the NCEP / GFS reproduced the seasonal variations of large-scale precipitation relatively well. Significant differences, however, are observed over central and eastern Pacific where the ITCZ precipitation is weaker / stronger in the reanalysis / the GFS climate model, respectively, compared to that in the two merged analyses.

#### 4. INTERANNUAL VARIABILITY

Monthly precipitation anomaly patterns associated with the ENSO and several other major atmospheric circulation patterns (Barnston and Livezey, 1987) are examined for the 23-year period from 1979 to 2001 when all of the 4 data sets are available.

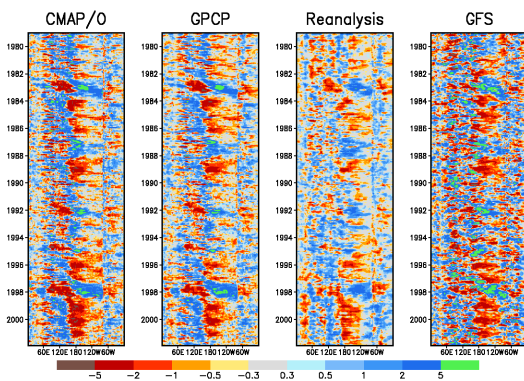


Fig. 3: Longitude-time section of monthly precipitation anomaly (mm/day) averaged over a tropical belt from 10°S-10°N over the Pacific Ocean, for the merged analyses of CMAP/O, and GPCP Version 2, and the outputs from the NCEP/NCAR reanalysis and the AMIP runs of the NCEP / GFS climate model.

Presented in fig.3 are Hovermoller diagrams of monthly precipitation anomaly (mm/day) averaged over the tropical belt from 10°S-10°N

as obtained from the CMAP/O (left), GPCP Version 2 (2<sup>nd</sup> from left), the reanalysis (3<sup>rd</sup> from left), and the NCEP/GFS (right). Anomaly patterns associated with the evolution of ENSO events over the tropical Pacific are well captured in both of the merged analyses. In general, both the reanalysis and the NCEP / GFS were able to reproduce these patterns reasonably well. Close examinations of the figure, however, reveal that the reanalysis precipitation present an eastward displacement compared to that in the merged analyses, while the NCEP / GFS exhibits smaller scale anomaly patterns that are not observed in the merged analyses.

To further investigate the interannual variations of large-scale precipitation associated with the ENSO, composite maps are constructed for the precipitation anomaly for warm and cold ENSO episodes during the 23-year period from 1979 to 2001. A simple approach is adopted here to declare a cold / warm ENSO episode if the seasonal mean SST anomaly over the NINO3.4 region exceeds  $-0.5/0.5^{\circ}\text{C}$ . Fig.4 shows the distributions of the differences observed during the warm and cold conditions for the DJF period.

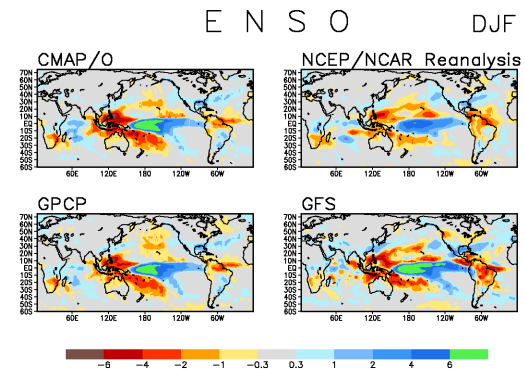


Fig. 4: Differences in DJF mean precipitation (mm/day) between warm and cold ENSO episodes during the 23-year period from 1979 to 2001, for the merged analyses of CMAP/O, and GPCP Version 2, and the outputs from the NCEP/NCAR reanalysis and the AMIP runs of the NCEP / GFS climate model.

As clear from the composite maps for the two merged analyses, during the DJF period, warm ENSO episodes are characterized by more precipitation over the central Pacific, southeastern South America, the extreme northeastern Pacific and adjacent coastal regions of North America, and over a belt extending from the eastern Pacific, across the Gulf of Mexico well into the Atlantic. Less than normal precipitation, meanwhile, is observed over the

western Pacific, the central Pacific away from the Tropics, Amazonia, and South Africa. The composite anomaly patterns produced by the reanalysis and the NCEP / GFS are very similar to those in the merged analyses. In the reanalysis, the maximum positive anomaly is located eastward and its magnitude is smaller than those in the merged analyses. In the NCEP / GFS, the magnitude of the precipitation is larger over most of the globe.

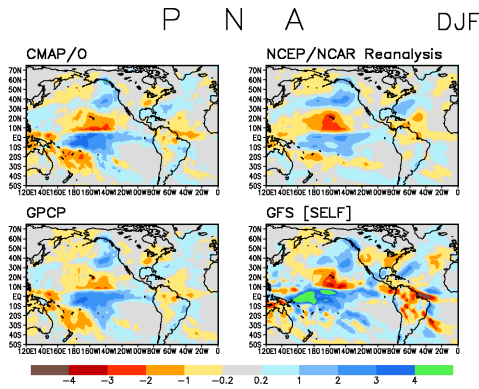


Fig. 5: Differences in DJF mean precipitation (mm/day) between high and low phases of the PNA during the 23-year period from 1979 to 2001, for the merged analyses of CMAP/O, and GPCP Version 2, and the outputs from the NCEP/NCAR reanalysis and the AMIP runs of the NCEP / GFS climate model.

To describe the interannual variations of large-scale precipitation associated with major atmospheric circulation patterns, DJF mean precipitation composites are constructed for the Pacific / North America (PNA) pattern, North Atlantic Oscillation (NAO), and the Arctic Oscillation (AO), respectively. Corresponding indices, calculated from circulation fields based on Barnston and Livezey (1987), are used to determine the phase of the temporal variations associated with these patterns. A DJF month is classified as in low / high phase if the normalized index exceeds  $-0.5 / 0.5$  times of its standard deviation. In constructing the composites for the precipitation fields for the two merged analyses and the NCEP reanalysis, the indices derived from the NCEP reanalysis circulation fields are employed. For the NCEP / GFS precipitation fields, the PNA, NAO and AO indices are calculated from its own atmospheric circulation fields.

During cold season, precipitation variations associated with the PNA (fig.5) are characterized by a series of anomaly patterns with alternating signs over Pacific, North America and Atlantic Ocean. These patterns extend northwardly from tropical central / western Pacific to the sub-

tropical North Pacific, the extreme northeastern Pacific, and then turn to east, reaching the North America Continent, and the northwestern Atlantic Ocean. Both the reanalysis and the GFS capture the precipitation variation patterns associated with the PNA very well, especially in the geological positions of these anomalies. Differences, however, exist in the magnitude of the anomalies, especially over tropical Pacific where the reanalysis and the GFS tend to produce weaker and stronger anomalies, respectively, compared to the two merged analyses.

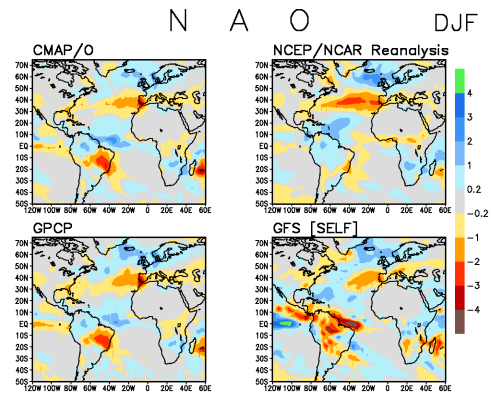


Fig. 6: As in figure 5, except for the NAO.

Anomalous precipitation patterns associated with the NAO (fig.6) are characterized by enhanced precipitation over northeastern Canada, Greenland, extending across the Atlantic to Northern Europe during high index periods, and over the Middle East, the Mediterranean, and the Atlantic Ocean between  $\sim 25^{\circ}\text{N} - 45^{\circ}\text{N}$  during the low index periods. This seesaw pattern of zonally oriented precipitation anomaly with alternating signs extends further south across the Equator to the northeastern portion of the South America. Both the reanalysis and the NCEP GFS were able to capture the precipitation variations associated with the NAO reasonably well north of the Equator. However, neither of them succeeded in reproducing the NAO-related precipitation anomaly over the Southern Hemisphere.

The high and low phases of the Arctic Oscillation (AO) are accompanied by precipitation anomalies organized in zonally oriented bands over mid- and high latitudes over the Northern Hemisphere (fig.7). During the high AO phase, maximum positive and negative precipitation anomalies are located over the Norwegian Sea and over western Spain and its adjacent Atlantic Ocean, respectively. The reanalysis reproduced the AO-related precipitation anomalies in close agreement with those in the merged analyses

both spatial distribution patterns and magnitude. The AO-related anomaly patterns generated by the NCEP / GFS climate model, meanwhile, are similar to those in the merged analyses.

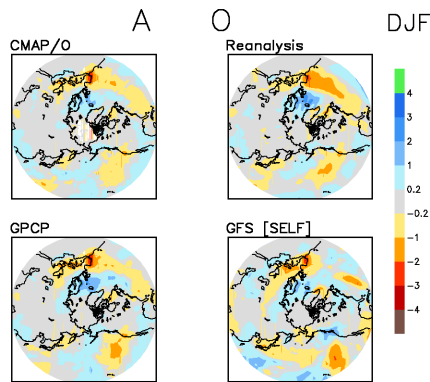


Fig. 7: As for in figure 5, except for the AO.

## 5. SUMMARY

Seasonal evolution and interannual variations of large-scale precipitation associated with ENSO, PNA, NAO and AO have been described using the CMAP and GPCP merged analyses for a 23-year period from 1979 to 2001;

The seasonal evolution and the anomaly patterns as observed in the merged analyses are compared with those in the precipitation fields produced by the NCEP/NCAR reanalysis and the NCEP / GFS climate model;

The two sets of the merged analyses, the CMAP/O and the GPCP Version 2, present seasonal and interannual variations of large-scale precipitation with very close agreements in both the patterns and magnitude. The reanalysis and the GFS climate model are able to reproduce these variations reasonably well but exhibit differences with the merged analyses in smaller scale features and in magnitude.

## REFERENCES

Adler, R.F., and Coauthors, 2003: The Version 2 Global Precipitation Climatology Project (GPCP) monthly precipitation analysis (1979 – present). *J. Hydrometeor.*, **4**, (in press).

Barnston, A.G., and R.E. Livezey, 1987: Classification, seasonality and persistence of low frequency atmospheric circulation patterns. *Mon. Wea. Rev.*, **115**, 1,083 – 1,126.

Gruber, A., X. Su, and J. Schemm, 2000: The comparison of two merged rain gauge –

satellite precipitation datasets. *Bull. Amer. Meteor. Soc.*, **81**, 2631 – 2644.

Huffman, and Coauthors, 1997: The Global Precipitation Climatology Project (GPCP) combined precipitation dataset. *Bull. Amer. Meteor. Soc.*, **78**, 5-20.

Kalnay, E., and Coauthors, 1996: The NCEP / NCAR 40-year Reanalysis Project. *Bull. Amer. Meteor. Soc.*, **77**, 437 – 472.

Wang, W., S. Saha, H-L. Pan, S. Nadiga, and G.White, 2003:Simulation of ENSO in the new NCEP Coupled Forecast System Model. *Bull. Amer. Meteor. Soc.*, (submitted).

Xie, P. and P. A. Arkin, 1997: Global precipitation: A 17-year monthly analysis based on gauge observations, satellite estimates and numerical model outputs. *Bull. Amer. Meteor. Soc.*, **78**, 2539-2558.